

Halmstad University submission to the *First ICB Competition on Iris Recognition (ICIR2013)*

Fernando Alonso-Fernandez, Josef Bigun
Intelligent Systems Lab (IS-Lab/CAISR), Halmstad University, Sweden
{feralo,josef.bigun}@hh.se

I. INTRODUCTION

With the pronounced need for reliable personal identification, iris recognition has become an important enabling technology in our society. Although an iris pattern is naturally an ideal identifier, the development of a high-performance iris recognition algorithm and transferring it from research lab to practical applications is still a challenging task. Automatic iris recognition has to face unpredictable variations of iris images in real-world applications. Therefore the first ICB Competition on Iris Recognition (or ICIR2013 shortly) is organized to track the state-of-the-art of iris recognition [1].

II. PROTOCOL OF THE COMPETITION

ICIR2013 is open to both academia and industry. There are two iris image databases used in ICIR2013 for training and testing purposes, respectively. The training database, CASIA-Iris-Thousand (Figure 1), contains 20,000 iris images of 1,000 subjects (20 images/subject and 10 images/eye). Prior to the evaluation, CASIA-Iris-Thousand was released to the participants to tune their algorithms. CASIA-Iris-Thousand was collected using the iris camera produced by IrisKing. All iris images of CASIA-Iris-Thousand are 8 bit gray-level BMP files and the image resolution is 640×480 . The testing database, IR-TestV1 (Figure 2), contains 10,000 iris images of 1,000 subjects (10 images/subject and 5 images/eye). IR-TestV1 was sequestered by the evaluation organizers to evaluate the competing algorithms. The iris images of IR-TestV1 were captured using IrisGuard camera in one session. The main sources of intra-class variations in IR-TestV1 are motion blur, non-linear deformation, eyeglasses and specular reflections. All iris images of IR-TestV1 are 8 bit gray-level BMP files and the image resolution is 640×480 .

All participants were allowed to submit two executables, one used to generate a feature template from an iris image (*enrollment* file), and another to match two iris feature templates (*matching* file). In addition, participants could also submit other supporting files along with the two executables. The *matching* file should output a matching score ranging from 0 to 1, or a value of -1 if the algorithm fails to match. If matching cannot be successfully implemented due to failure to enrollment or failure to match, a random variable ranging from 0 to 1 is assigned as the matching score. Each participant were allowed to submit up to three algorithms. The organizers only accepted qualified iris recognition algorithms which met the following requirements due to limited competition resources:

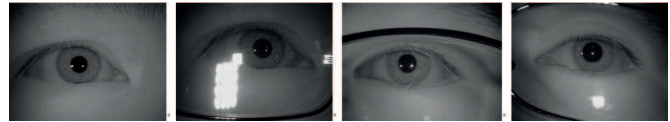


Fig. 1. Example of iris images from the ICIR2013 training database (CASIA-Iris-Thousand).

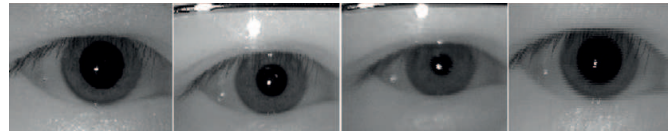


Fig. 2. Example of iris images from the ICIR2013 testing database (IR-TestV1).

the Equal Error Rate (EER) must be less than 5% on the training database, the average processing time for feature encoding must be less than 3 seconds and the average matching time must be less than 0.1 seconds on a normal personal computer.

All possible intra-class comparisons were implemented with the testing database to obtain the false non-match rate (FNMR), providing a total of 20,000 intra-class match results. Also, one sample was selected from each iris class to evaluate the false match rate (FMR) so there were 1,999,000 inter-class match results. Popular performance metrics of iris recognition such as FNMR, FMR, EER and ROC were reported and the metric $F4(\text{FNMR} @ \text{FMR}=0.0001)$ was used to rank the performance of submitted algorithms.

III. HALMSTAD UNIVERSITY IRIS RECOGNITION ALGORITHM

A. Image preprocessing

Specular reflections can interfere with the detection of iris boundaries, especially when reflections are close to them. We therefore start with removing specular reflections with the method presented in [2]. For better accuracy, histogram equalization is carried out first, so the darkest pixels are mapped to the lowest regions of the histogram. To aid in pupil search, we also pre-estimate the pupil area by thresholding, since the pupil is generally darker than surrounding areas. The whole process is shown in Figure 3.

B. Pupil detection

In this task, we search for an estimation of the pupil boundary. This is done using the method proposed in [3]. Assuming

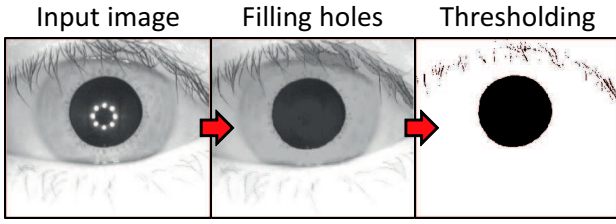


Fig. 3. Removal of specular reflections and coarse pupil detection.

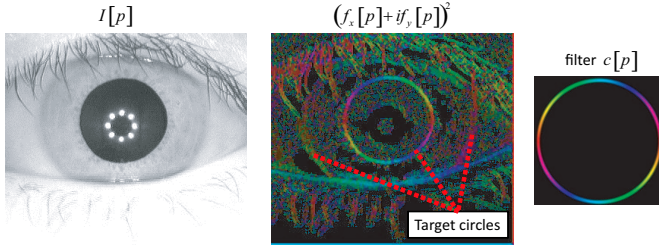


Fig. 4. Iris segmentation using the Generalized Structure Tensor (GST). Functions $f_x[p]$, $f_y[p]$ are the partial derivatives of the image $I[p]$ at pixel $p = [x, y]$, and $c(p)$ is a complex circular filter encoding local orientations of the sought pattern. The hue in $(f_x(p) + i f_y(p))^2$ and $c(p)$ encodes the direction and the saturation represents the complex magnitude. To depict the magnitude, they are re-scaled so that maximum saturation represents the maximum magnitude and black represents zero magnitude.

that iris detection can be started with a circular detector [4], [2], [5], it can be done by means of the Generalized Structure Tensor [6]. For this purpose, a circular complex filter $c(p)$ encoding local orientations is used, see Figure 4. Image $(f_x(p) + i f_y(p))^2$, built from the estimated partial derivatives $f_x[p]$, $f_y[p]$ of an iris image $I[p]$, is convolved with $c(p)$ as follows:

$$I_{20} = \sum_p c(p) (f_x(p) + i f_y(p))^2 \quad (1)$$

Pupil boundary detection is done as depicted in Figure 5. We search for the pupil boundary with a circular filter $c(p)$ of variable radius. For each radius, the maximum magnitude of I_{20} is recorded, and the image position where it occurs. Maxima detection is only done in pixels of the pupil area pre-estimated in the previous step. It can be shown that a high response in $|I_{20}|$ and zero argument of I_{20} is obtained at a point p if there are edges at the prescribed (same) distance from p and there is an agreement in terms of local orientations (structure tensors) with those of the circle. Thus, a peak in $|I_{20}|$ will be obtained when the radius of the circular filter fits that of the pupil boundary. When it happens, $|I_{20}|$ shows high values only in a small neighborhood around the pupil center. After this detection procedure, we obtain the center and radius of the circle that approximates the pupil boundary. As shown below, the feature extractor does not need information concerning the sclera boundary, allowing computational time savings.

Filter $c(p)$ is an example of symmetry filters [6], designed to detect points that poses a certain symmetry type (circular, parabolic, linear, etc.). Symmetry filters have been successfully applied to a wide range of detection tasks such as cross-markers in vehicle crash tests [7], core-points and minutiae in fingerprints [8], [9], eyes in face images [10], and recently

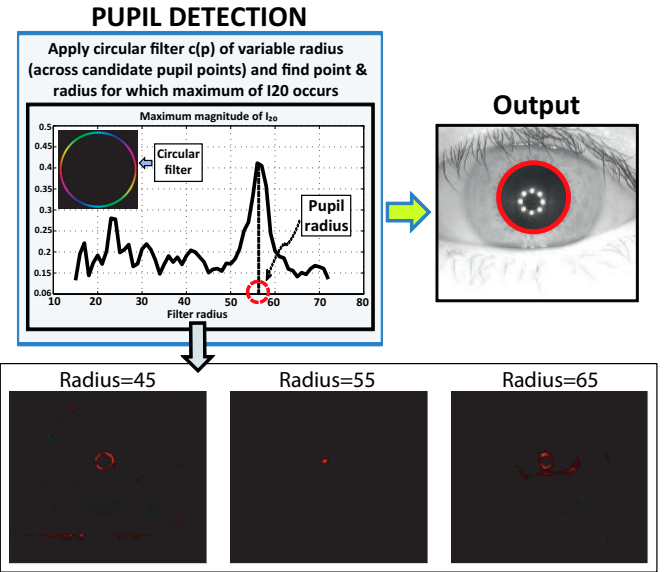


Fig. 5. Top: System model for iris segmentation using the Generalized Structure Tensor. Bottom: Tensor I_{20} for different radii of the circular saturation $c(p)$. The hue in the images encodes the direction and the saturation represents the magnitude of complex numbers. To depict the magnitude, it is re-scaled so that maximum saturation represents the maximum magnitude of I_{20} and black represents $I_{20} = 0$.

iris boundaries [3]. The beauty of this method is that, apart from a correlation of edge magnitudes, it takes into account the direction of edges. By using complex filters encoding local orientations of the sought pattern, its response is penalized if there is disagreement of local orientations of the image with those of the filter. This is achieved because $c(p)$, as defined in Equation 1, encodes the opposite direction of the sought pattern, so if the image and filter orientations “agree”, they are canceled during the complex convolution (thus, the zero argument expected in I_{20}). This is not exploited by other edge-based detection methods such as the Circular Hough Transform or the Integro-Differential operator, where all boundary pixels contribute equally to (do not penalize) the detection of circles. Indeed, the Generalized Structure Tensor can be seen as a (Generalized) Hough Transform with the additional capability of recognize anti-targets *during* the target recognition [6].

C. Feature extraction and matching

We use two feature extraction algorithms. The first one is based on the Gabor spectral decomposition proposed in [11], while the second one is based on the SIFT operator [12].

In the first algorithm, input images are analyzed with an square retinotopic sampling grid, which is positioned in the pupil center (Figure 6, left). The grid has 117 points, distributed uniformly in 9 rows and 13 columns. Dimensions of the rectangular grid are fixed. Its width is set to three times the average pupil radius of the images of the training database (CASIA-Iris-Thousand). The average pupil radius of CASIA-Iris-Thousand is obtained by running the detection algorithm of the previous section. Height of the rectangular grid is 4/6 of its width [13]. The local power spectrum of the image is

then sampled at each point of the grid by a set of Gabor filters (Figure 6, right). We use 30 Gabor filters, organized in 5 frequency channels and 6 equally spaced orientation channels. Filter wavelengths span the range from 4 to 16 pixels in half-octave intervals. Development experiments has shown that there is not a significant drop in accuracy using only the lowest frequency channel. Thus, for speed purposes, only this channel is extracted in our system. The Gabor responses are grouped into a single complex vector, which is used as identity model. Matching between two images is done using the magnitude of complex values. Prior to matching, magnitude vectors are normalized to a probability distribution (PDF), and matching is done using the χ^2 distance [14]. No rotation compensation is done between query and test iris images. As demonstrated in [11], this does not have significant impact in the performance, allowing additional time savings.

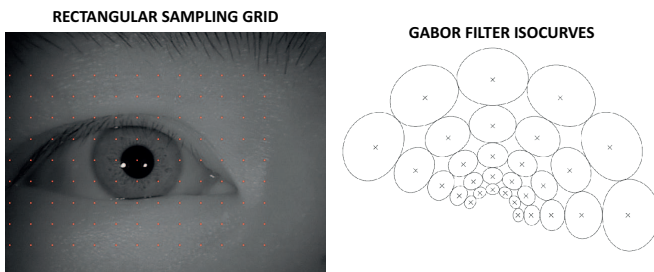


Fig. 6. **Left:** Rectangular sampling grid. **Right:** Iso-curves of Gabor filters.

For the matcher based on the SIFT operator, we use a free implementation of the SIFT algorithm¹, with the adaptations for iris images described in [15]. SIFT keypoints are extracted only in the region given by the square retinotopic sampling grid defined above. The recognition metric is the number of matched keypoints between two iris images, normalized by the mean number of detected keypoints in each of the two images. Figure 7 shows an example of matching between two iris images using this system (image from [15]).

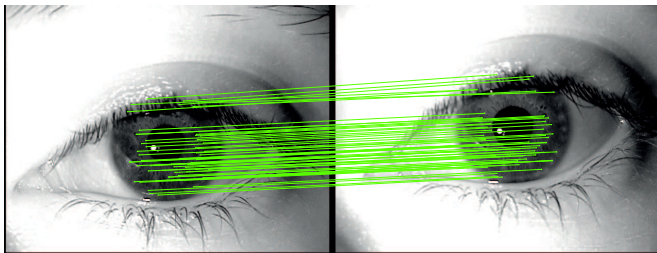


Fig. 7. Matching of two iris images using the SIFT operator.

D. System fusion

Scores of the two systems are then fused to obtain a single score. For the fusion experiments, we use linear logistic regression fusion. Given N matchers which output the scores $(s_{1j}, s_{2j}, \dots, s_{Nj})$ for an input trial j , a linear fusion of these scores is: $f_j = a_0 + a_1 \cdot s_{1j} + a_2 \cdot s_{2j} + \dots + a_N \cdot s_{Nj}$.

¹<http://vision.ucla.edu/vedaldi/code/sift/assets/sift/index.html>

The weights a_0, a_1, \dots, a_N are trained via logistic regression following the procedure described in [16]. This training is done using intra- and inter-class matching scores from the training database (CASIA-Iris-Thousand). We use this trained fusion approach because it has shown better performance than simple fusion rules (like the mean or the sum rule) in previous works [17], [16]. Scores are finally normalized to the 0-1 range by using min-max normalization.

IV. SUMMARY OF COMPETITION RESULTS

A total of 13 algorithms from 8 participants were submitted to ICIR2013. Participants were from 6 different countries (Brazil, China, France, India, Japan and Sweden). Table I gives the performance of the three winning algorithms, as reported in the website of the competition [1] (only the best three algorithms have been publicly reported in the web). A joint paper between all participants of the competition is planned, where all submitted algorithms will be described in detail. At the end of this document, it is also annexed the Algorithm Evaluation Report of the Halmstad University Iris Recognition Algorithm, as released by the organizers.

REFERENCES

- [1] ICIR2013, "First ICB Competition on Iris Recognition - <http://iris.idealtest.org/2013/icir2013.jsp>." 2013.
- [2] Z. He, T. Tan, Z. Sun, and X. Qiu, "Toward accurate and fast iris segmentation for iris biometrics," *IEEE Trans. on Pattern Analysis and Machine Intelligence*, vol. 31, no. 9, pp. 1295–1307, 2009.
- [3] F. Alonso-Fernandez and J. Bigun, "Iris boundaries segmentation using the generalized structure tensor: an study on the effects of image degradation." *Proc. IEEE Conference on Biometrics: Theory, Applications and Systems, BTAS, Washington DC (USA)*, 2012.
- [4] J. Daugman, "New methods in iris recognition," *IEEE Trans. on Systems, Man and Cybernetics, part B: Cybernetics*, vol. 37, no. 5, pp. 1167–1175, 2007.
- [5] D. Jeong, J. Hwang, B. Kang, K. Park, C. Won, D.-K. Park, and J. Kim, "A new iris segmentation method for non-ideal iris images," *Image and Vision Computing*, vol. 28, no. 2, pp. 254–260, 2010.
- [6] J. Bigun, *Vision with Direction*. Springer, 2006.
- [7] J. Bigun, G. Granlund, and J. Wiklund, "Multidimensional orientation estimation with applications to texture analysis and optical flow," *IEEE Trans. on Pattern Analysis and Machine Intelligence*, vol. 13, no. 8, pp. 775–790, August 1991.
- [8] K. Nilsson and J. Bigun, "Localization of corresponding points in fingerprints by complex filtering," *Pattern Recognition Letters*, vol. 24, pp. 2135–2144, 2003.
- [9] H. Fronthaler, K. Kollreider, J. Bigun, J. Fierrez, F. Alonso-Fernandez, J. Ortega-Garcia, and J. Gonzalez-Rodriguez, "Fingerprint Image Quality Estimation and its Application to Multi-Algorithm Verification," *IEEE Trans. on Information Forensics and Security*, vol. 3, no. 2, pp. 331–338, 2008.
- [10] D. Teferi and J. Bigun, "Multi-view and multi-scale recognition of symmetric patterns," *Proc. Scandinavian Conference on Image Analysis, SCIA*, vol. LNCS-5575, pp. 657–666, 2009.
- [11] F. Alonso-Fernandez and J. Bigun, "Periocular recognition using retinotopic sampling and gabor decomposition," *Proc. Whats in a Face?, WIAF, in conjunction with European Conference on Computer Vision, ECCV, Florence, Italy*, 2012.
- [12] D. Lowe, "Distinctive image features from scale-invariant key points," *International Journal of Computer Vision*, vol. 60, no. 2, pp. 91–110, 2004.
- [13] U. Park, R. R. Jillela, A. Ross, and A. K. Jain, "Periocular biometrics in the visible spectrum," *IEEE Transactions on Information Forensics and Security*, vol. 6, no. 1, pp. 96–106, 2011.
- [14] A. Gilperez, F. Alonso-Fernandez, S. Pecharroman, J. Fierrez, and J. Ortega-Garcia, "Off-line signature verification using contour features," *Proc. International Conference on Frontiers in Handwriting Recognition, ICFHR*, 2008.

Rank	Organization	Country	FNMR@FMR=0.0001	EER
1	Zhuhai YiSheng Electronics Technology Co. Ltd	China	7.09%	2.75%
2	University of Halmstad	Sweden	9.24%	3.19%
3	Institut Fresnel (CNRS UMR 7149)	France	42.16%	9.33%

TABLE I
ICIR2013 RESULTS OF THE BEST THREE ALGORITHMS [1].

- [15] F. Alonso-Fernandez, P. Tome-Gonzalez, V. Ruiz-Albacete, and J. Ortega-Garcia, "Iris recognition based on sift features," *Proc. IEEE Intl. Conf. on Biometrics, Identity and Security, BIDS*, 2009.
- [16] F. Alonso-Fernandez, J. Fierrez, D. Ramos, and J. Gonzalez-Rodriguez, "Quality-based conditional processing in multi-biometrics: Application to sensor interoperability," *IEEE Trans. on Systems, Man and Cybernetics-Part A: Systems and Humans*, vol. 40, no. 6, pp. 1168–1179, 2010.
- [17] F. Alonso-Fernandez, J. Fierrez, D. Ramos, and J. Ortega-Garcia, "Dealing With Sensor Interoperability in Multi-biometrics: The UPM Experience at the Biosecure Multimodal Evaluation 2007," *Defense and Security Symposium, Biometric Technologies for Human Identification, BTHI, Proc. SPIE*, vol. 6944, pp. 69 440J1–69 440J12, 2008.

**The First ICB Competition on Iris Recognition
(ICIR2013)**

Algorithm Evaluation Report

ID: 08
Submitter: Fernando Alonso-Fernandez & Josef Bigun
Organization: University of Halmstad
Country: Sweden

Reported by
Institute of Automation, Chinese Academy of Sciences
May 30th, 2013

Introduction

With the pronounced need for reliable personal identification, iris recognition has become an important enabling technology in our society. Although an iris pattern is naturally an ideal identifier, the development of a high-performance iris recognition algorithm and transferring it from research lab to practical applications is still a challenging task. Automatic iris recognition has to face unpredictable variations of iris images in real-world applications. Therefore the first ICB Competition on Iris Recognition (or ICIR2013 shortly) is organized to track the state-of-the-art of iris recognition.

ICIR2013 is open to both academia and industry. A public platform, the Biometrics Ideal Test (BIT; <http://biometrics.idealtest.org>) is used to organize the competition. Until March 20, 2013, there are total 13 algorithms submitted by 8 participants, who are from Brazil, China, France, India, Japan and Sweden. Each participant can maximally submit three algorithms, and the one of best performance is selected for competition.

Database Information

	Training	Testing
Database Name	CASIA-Iris-Thousand	ir_testv1
Number of subjects	1,000	1,000
Number of classes	2,000	2,000
Number of images	20,000	10,000

Match Information

intra-class match	20,000
inter-class match	1,999,000
DI	2.3565

Match Result

	EER	0.0319
FMR	When FNMR ≤ 0	1.0000
FNMR	When FMR ≤ 0	0.9882
	When FMR $\leq 1/100$	0.0577
	When FMR $\leq 1/1000$	0.0726
	When FMR $\leq 1/10000$	0.0924

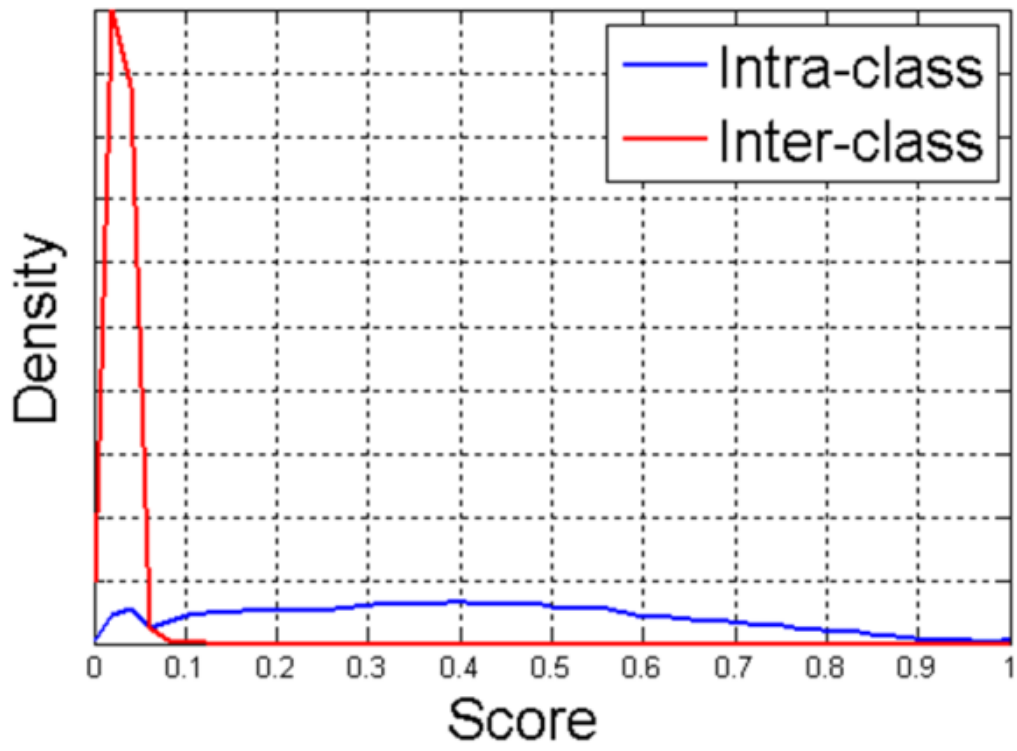


Figure 1 Score distributions

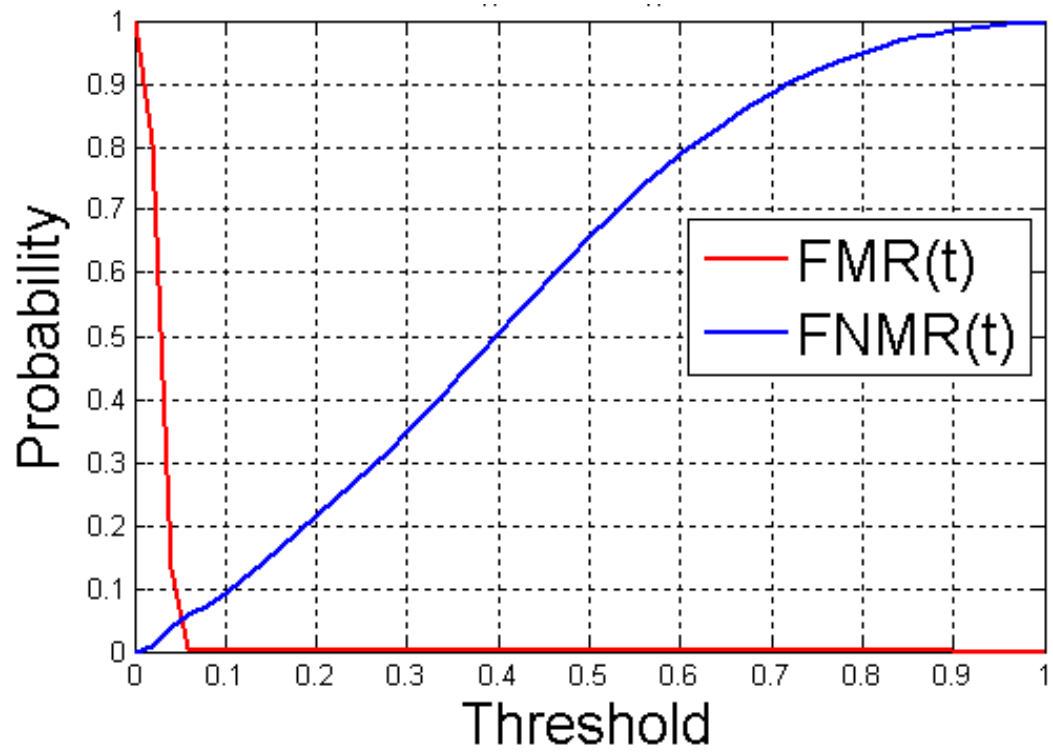


Figure 2 FMR(t) and FNMR(t) graphs

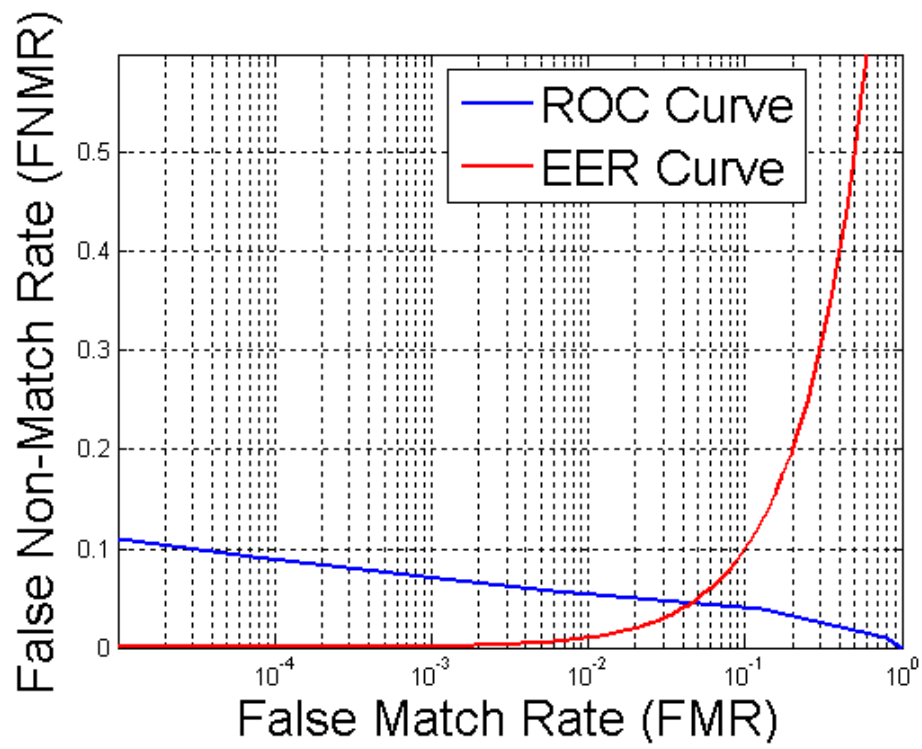


Figure 3 ROC curves